Circuit Simulation of Magnetization Dynamics and Spin Transport

Article *in* IEEE Transactions on Electron Devices · May 2014

DOI: 10.1109/TED.2014.2305987

CITATIONS
29

READS
164

8 authors, including:

Rouhollah Mousavi Iraei
Georgia Institute of Technology
13 PUBLICATIONS **103** CITATIONS

SEE PROFILE

Shaloo Rakheja
University of Illinois, Urbana-Champaign
100 PUBLICATIONS **538** CITATIONS

SEE PROFILE

Dmitri Evgenievich Nikonov
Intel
255 PUBLICATIONS **6,665** CITATIONS

SEE PROFILE

Circuit Simulation of Magnetization Dynamics and Spin Transport

Phillip Bonhomme, *Member, IEEE*, Sasikanth Manipatruni, Rouhollah M. Iraei, Shaloo Rakheja, Sou-Chi Chang, Dmitri E. Nikonov, *Senior Member, IEEE*, Ian A. Young, *Fellow, IEEE*, and Azad Naeemi, *Senior Member, IEEE*

***Abstract*— In this paper, compact circuit models for spintronic devices have been developed by manipulating the underlying physical equations. We have simulated, via circuit simulation: 1) the magnetization dynamics governed by the Landau–Lifshitz–Gilbert (LLG) equation and 2) the spin transport physics governed by the spin drift–diffusion equation. The models have been validated using numerical and analytical solutions of the LLG equation and the spin drift–diffusion equations, respectively. Simulations of an all-spin logic device demonstrate the applications of the developed models in device and circuit simulation.**

***Index Terms*— Circuit theory, modeling, magnetoelectronics, spin polarized transport.**

I. Introduction

SPINTRONIC devices utilize the properties of an electron's spin as a novel state variable for information storage, manipulation, and communication. Recent interest in spintronic devices is due to their potential as a low-power CMOS process compatible computing devices [1], [2]. To leverage spintronic devices in circuit designs, compact circuit models of spin physics will be essential. Developing compact circuit models will require an understanding of the underlying physics governing spintronic devices.

In the case of spintronic devices, the underlying physics are well understood. The key interaction between spins in a spintronic device involves storing spin in a ferromagnetic body, and then transferring the angular momentum through a nonmagnetic conductor into another ferromagnet. The physical behavior and resulting circuit theory of spintronic devices are detailed in [2]–[9]. The physics governing the magnetization of the ferromagnetic body are predicted by the Landau–Lifshitz Gilbert (LLG) equation [10], [11]. The transport properties of spin in a nonmagnetic conductor are governed by the spin drift–diffusion equation [12], [13]. The mathematical relationship between the spin voltages and currents defined in [4] connects the physical quantities of spin storage in the ferromagnet to spin transport in the nonmagnetic conductor. When coupled together, these equations form the basis for the simulation of spintronic devices.

Simulations of spintronic devices have been performed in [1], [14], and [15]. In [14], a complete analysis of a ferromagnetic/nonmagnetic stacked structure is performed *ab initio* using quantum mechanical methods. While this model simulates all of the dynamics previously mentioned, it does not enable the development of a compact model suitable for circuit simulation. Reference [1] solves the LLG equation and the steady-state spin transport equations by coupling the initial and boundary conditions of the relevant differential equations. This is accomplished by solving the magnetization dynamics in the time domain for one time step, Δt, then passing the solution as a boundary condition to the spin transport equations. This approach ignores the transient characteristics involved in the spin transport physics. In [15], a compact circuit model simulates the LLG equation in ferromagnets, but this model only simulates a single type of spintronic device, the magnetic tunnel junction (MTJ). The MTJ is formed by stacking an insulating material with ferromagnetic elements. In the interest of designing a broader class of spintronic devices, we would like to be able to simulate spin transport in a nonmagnetic channel, something this model does not simulate.

In the process of developing compact circuit simulation compatible models, we will seek to link the magnetization dynamics to the spin transport physics using the results obtained in [16]. In [16], the magnetization, $\vec{m}$, is linked to the spin transport quantities, $\overline{I}_s$ and $\overline{V}_s$, through a matrix–vector product. The main contribution of this paper will be compact circuit models that are developed by mapping the equations governing the magnetization dynamics (the LLG equation), the spin transport physics (the spin drift–diffusion equation), and the connection between the two, spin injection, to equivalent circuits.

In this paper, we seek to create a unified cohesive device and circuit simulation environment using basic electrical circuit elements, such as resistors, capacitors, and current sources. This approach enables an easy construction and simulation of an equivalent circuit model for spintronic devices using a

Manuscript received November 4, 2013; revised December 26, 2013; accepted January 28, 2014. Date of publication March 28, 2014; date of current version April 18, 2014. This work was supported by Intel MSR under Contract 2011-IN-2198. The review of this paper was arranged by Editor R. K. Lake.

P. Bonhomme, R. M. Iraei, S.-C. Chang, and A. Naeemi are with the School of Electrical and Computer Engineering, Georgia Institute of Techology, Atlanta, GA 30332 USA (e-mail: bonhomme@gatech.edu; ruhollah.musavi@gmail.com; souchi@gatech.edu; azad@gatech.edu).

S. Manipatruni, D. E. Nikonov, and I. A. Young are with the Components Research Group, Intel Corporation, Hillsboro, OR 97124 USA (e-mail: sasikanth.manipatruni@intel.com; dmitri.e.nikonov@intel.com; ian.young@intel.com).

S. Rakheja is with Microsystems Technology Laboratories, Massachusetts Institute of Technology, Cambridge, MA 02139 USA (e-mail: shaloo.rakheja@gatech.edu).

Color versions of one or more of the figures in this paper are available online at http://ieeexplore.ieee.org.

Digital Object Identifier 10.1109/TED.2014.2305987

circuit solver, such as HSPICE [17]. The circuit simulator can solve all underlying physical equations simultaneously with no need for going back and forth between numerical solvers. The circuit elements also provide intuition and insight into the operation of these emerging devices.

The rest of this paper is organized as follows. In Section II, we derive all of the equations in the forms that can be directly mapped to equivalent circuit models. The models are then validated in Section III by comparing the simulation results to solutions of the physical equations. In Section IV, we discuss important observations that we have made concerning the models.

II. Development of Compact Spintronic Models

Section II-A covers the derivation of the circuit model for the magnetization dynamics. In Section II-B, we cover the spin injection physics, and in Section II-C, we derive the equations for the spin transport physics. The dependent variables of these equations are then mapped to circuit nodes and branches, creating a compact circuit model that enables the simulation of spintronic devices.

A. Development of a SPICE Equivalent Circuit for the LLG Equation

The LLG equation models the temporal evolution of the magnetization dynamics within a ferromagnet. The LLG equation describes the change in magnetization in a ferromagnet as a function of the torque applied to the magnetization [18]. The torque includes the effect of the internal field, the thermal field, the damped motion, and spin-transfer torque [4]

$$\frac{d\vec{m}}{dt} = -\gamma\,\mu_0\big(\vec{m}\times\big(\vec{H}+\vec{H}_T\big)\big)+\alpha\left(\vec{m}\times\frac{d\vec{m}}{dt}\right)+\frac{\vec{I}_{s,\perp}}{qN_s}$$

where γ is the gyromagnetic ratio, μ_0 is the free space permeability, α is the Gilbert damping coefficient, q is the unit charge, and N_s is the number of spins in the ferromagnet.

The internal field of the ferromagnet includes the effect of the uniaxial anisotropy field and the demagnetization field. The uniaxial anisotropy field is determined by the crystal structure of the ferromagnetic material

$$\vec{H} = H_k m_z \hat{z} \tag{1}$$

where H_k is the Stoner–Wohlfarth field and depends on the energy density, K_u, of the ferromagnetic material

$$H_k = \frac{2K_u}{\mu_0 M_s}. \tag{2}$$

The demagnetization field depends on the demagnetization factors, $\overline{\mathbf{N}}_d$, and the saturation magnetization, M_s

$$\vec{H} = M_s\overline{\mathbf{N}}_d\vec{m} \tag{3}$$

where $\overline{\mathbf{N}}_d$ depends on the shape of the ferromagnetic body [19].

The thermal field is due to the thermal motion of electrons and is statistical in nature. The joint distribution of the thermal field according to the theory developed by [20] is Gaussian with mean

$$\langle\vec{H}_{T,i}(t)\rangle = 0. \tag{4}$$

The correlation between the components of $\vec{H}_T$ is defined over time interval τ as

$$\langle\vec{H}_{T,i}(t)\vec{H}_{T,j}(t+\tau)\rangle = \frac{2k_bT\alpha}{\gamma\,V\mu_0^2M_s}\delta_{ij}\delta(\tau). \tag{5}$$

Spin-transfer torque within a ferromagnet is due to the transfer of angular momentum initiated by applying a spin current. This spin polarized current is assumed to pass into the ferromagnet and dissipate within the ferromagnet. The direction of the spin-transfer torque is determined by the perpendicular component of the applied spin current, $\vec{I}_s$, relative to the magnetization, $\vec{m}$

$$\vec{I}_{s,\perp} = \vec{m}\times\big(\vec{I}_s\times\vec{m}\big). \tag{6}$$

The magnitude of the spin-transfer torque is determined by the ratio of the perpendicular spin current and the number of spin polarized electrons in the magnet, $\vec{I}_{s,\perp}/qN_s$.

The circuit model for the magnetization dynamics emulates the mathematical behavior of the LLG equation. The LLG equation can be refactored into an explicit form

$$N_sq(1+\alpha^2)\frac{dm_x}{dt} = f(\vec{m},\vec{I}_s,\vec{H}) \tag{7a}$$

$$N_sq(1+\alpha^2)\frac{dm_y}{dt} = g(\vec{m},\vec{I}_s,\vec{H}) \tag{7b}$$

$$N_sq(1+\alpha^2)\frac{dm_z}{dt} = h(\vec{m},\vec{I}_s,\vec{H}) \tag{7c}$$

where the right-hand side does not depend on the temporal derivative of $\vec{m}$. The LLG equation is refactored by expanding the cross products into a system of equations, and solving the resulting system for $dm_x/dt, dm_y/dt, dm_z/dt$. The refactored equation is of the form $Cdv/dt = i_c$, which expresses the current through a capacitor as a function of the voltage across it. The equivalent circuit for the LLG equation can be obtained by converting the three coupled differential equations, (7), into an equivalent circuit with capacitors and cross-coupled current sources, as shown in Fig. 1, where $C = 1/(1V)qN_s(1+\alpha^2)$ [F], $v = \vec{m}(1V) \equiv \vec{V}_m$ [V], and $i_c = f(\vec{V}_m/(1V),\vec{I}_s,\vec{H}), g(\vec{V}_m/(1V),\vec{I}_s,\vec{H}), h(\vec{V}_m/(1V),\vec{I}_s,\vec{H})$ [A]. This circuit also includes dependent voltage sources to model the internal fields, $\vec{H}$ and $\vec{H}_T$. The value of the voltage sources is determined by (1), (3), and (5), where the noise term is calculated by SPICE to have a Gaussian distribution with mean, zero, and amplitude, $\big(2k_bT\alpha/\gamma\,V\mu_0^2M_s\,\Delta t\big)^{1/2}$.

B. Spin Injection

Charge and spin currents can be calculated using the two-channel resistor model [14], [21]. The two-channel resistor model incorporates collinear ferromagnetic elements into circuit devices. The two-channel resistor model simulates the flow of a majority spin current $I_\uparrow$ and a minority spin current $I_\downarrow$. The majority and minority currents are determined

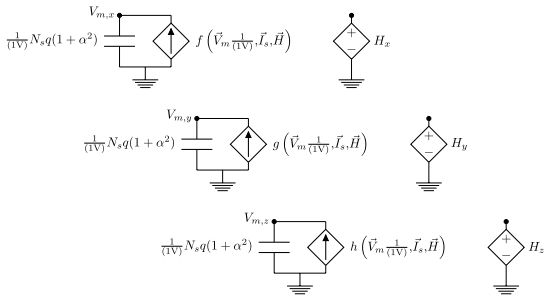

Fig. 1. Equivalent circuit model for spin storage.

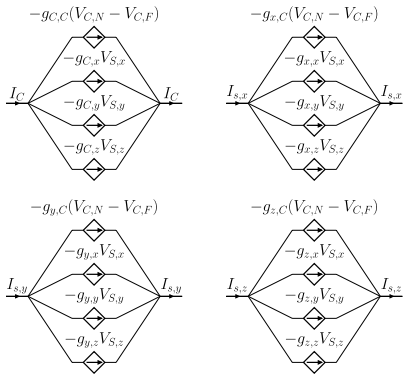

Fig. 2. Equivalent circuit model for spin injection (assuming the spin accumulation in the ferromagnet is 0: $V_s = V_{s,N} - V_{s,F} = V_{s,N}$).

by the majority and minority spin conductances of the material, $G_\uparrow$ and $G_\downarrow$, respectively. The total current $I_C = I_\uparrow + I_\downarrow$ can be calculated by conventional circuit analysis of the two-channel model

$$\begin{aligned} I_C &= G_\uparrow\big(V_{C,N} + \vec{V}_s \cdot \vec{m} - V_{C,F}\big) \\ &\quad + G_\downarrow\big(V_{C,N} - \vec{V}_s \cdot \vec{m} - V_{C,F}\big) \end{aligned} \tag{8}$$

where $\vec{V}_s$ is the spin voltage and is defined by the spin quasi-chemical potential $V_s = \mu_s/q$ for the x, y, and z components. The spin current $I_s = I_\uparrow - I_\downarrow$ is parallel to the magnetization and can be calculated using conventional circuit analysis of the two-channel (parallel) model

$$\begin{aligned} \vec{I}_{s,\parallel} = \vec{m} \cdot \big[&G_\uparrow(V_{C,N} + \vec{V}_s \cdot \vec{m} - V_{C,F}) \\ &- G_\downarrow(V_{C,N} - \vec{V}_s \cdot \vec{m} - V_{C,F})\big]. \end{aligned} \tag{9}$$

Ferromagnets with noncollinear states, $\vec{m}_1 \neq \pm\vec{m}_2$, lead to spin currents with transverse components. The transverse spin current, $\vec{I}_{s,\perp}$, is composed of an in-plane component proportional to $\big(\vec{V}_s \times \vec{m}\big)$, and an out of plane component proportional to $\vec{m} \times \big(\vec{V}_s \times \vec{m}\big)$. The transverse spin current can be calculated using the spin-mixing conductance [14], $G_{\uparrow\downarrow}$

$$\vec{I}_{s,\perp} = 2\mathrm{Re}G_{\uparrow\downarrow}\vec{m} \times \big(\vec{V}_s \times \vec{m}\big) + 2\mathrm{Im}G_{\uparrow\downarrow}\vec{V}_s \times \vec{m}. \tag{10}$$

The spin-mixing conductance depends on the scattering properties of a ferromagnet/nonmagnetic interface [22].

The complete relationship between the magnetization, $\vec{m}$, the charge current, I_C, the spin current, $\vec{I}_s$, the charge voltage, V_C, and the spin voltage, $\vec{V}_s$, can be described using tensor quantities

$$\begin{aligned} \overline{V}_s(t) &= [\, V_C \quad V_{s,x} \quad V_{s,y} \quad V_{s,z} \,]^T \\ \overline{I}_s(t) &= [\, I_C \quad I_{s,x} \quad I_{s,y} \quad I_{s,z} \,]^T. \end{aligned} \tag{11}$$

The total tensor current, $\overline{I}_s$, can be calculated as a function of $\vec{m}$, $G_\uparrow$, $G_\downarrow$, $G_{\uparrow\downarrow}$, and $\overline{V}_s$. The matrix–vector product that defines $\overline{I}_s$ is given in [4]

$$\overline{I}_s = \mathbf{G}_{\vec{m}}\overline{V}_s. \tag{12}$$

The vector description of $\overline{I}_s$ and $\overline{V}_s$ enables the development of a circuit model for spin injection. The circuit model for spin injection contains parallel current sources that mimic the matrix–vector product of (12). The matrix $\mathbf{G}_{\vec{m}}$ is computed symbolically and determines the conductance of the behavioral sources used in the circuit model of Fig. 2. Each cluster of four current sources represents the total current for each component of the $\overline{I}_s$ tensor as a function of both $\mathbf{G}_{\vec{m}}$ and $\overline{V}_s$.

C. Development of a SPICE Equivalent Circuit Model for Spin Transport

The drift–diffusion equations model the transport of charge and spin in nonmagnetic conductors. The charge diffusion equation is the continuity equation, where I_C is the current due to diffusion current only

$$\begin{aligned} C_e\frac{\partial V_C}{\partial t} &= \frac{\partial I_C}{\partial x} \\ I_C &= \sigma A\frac{\partial V_C}{\partial x} \end{aligned} \tag{13}$$

where C_e is the electrostatic capacitance per unit length, σ is the conductivity of the nonmagnetic conductor, and A is the cross-sectional area. This equation results in the familiar circuit model for an RC interconnect of an infinitesimal length shown in the upper left corner of Fig. 3. The spin drift–diffusion equation in a nonmagnetic conductor, along the x-axis, is the continuity equation for the spin accumulation [23], [24]

$$\frac{\partial \vec{s}}{\partial t} = \frac{1}{q}\frac{\partial \vec{J}_s}{\partial x} - \frac{\vec{s}}{\tau_s} \tag{14}$$

where the spin current density, $\vec{J}_s$, is due to both drift and diffusion currents

$$\vec{J}_s = q\mu E\vec{s} + qD\frac{\partial \vec{s}}{\partial x}. \tag{15}$$

The scalar x, y, and z components of the spin accumulation are functions of the corresponding scalar components of the spin quasi-chemical potential, μ_s, and the density of states

$$s_i = \mu_{s,i}\frac{\partial n_0}{\partial \eta} \tag{16}$$

where η is the chemical potential and n_0 is the carrier concentration. Substituting $\mu_s = qV_s$ into (16) and then dividing by V_s

$$\begin{aligned} s_i &= V_{s,i}q\frac{\partial n_0}{\partial \eta} \\ \frac{qs_i}{V_{s,i}} &= q^2\frac{\partial n_0}{\partial \eta} \equiv C_q \end{aligned} \tag{17}$$

where we have recognized the result as C_q, the quantum capacitance per unit volume.

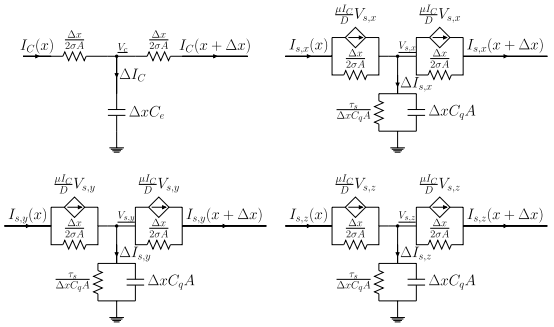

Fig. 3. Equivalent circuit model for spin transport (nonmagnetic conductor of length Δx).

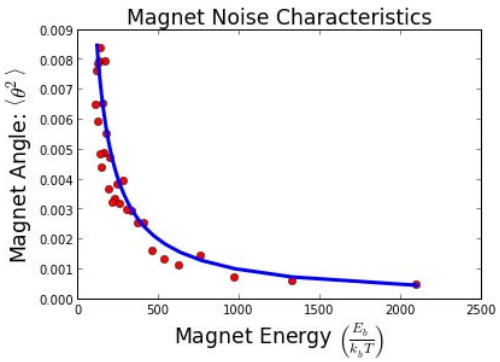

Fig. 4. Ferromagnet noise analysis. Red symbols: the circuit simulations. Blue curve: the solution of 20.

If we invoke Einstein's relation $\sigma = q^2 D \partial n_0/\partial \eta$, we can write the quantum capacitance as $C_q = \sigma/D$. We can also substitute the spin accumulation, $\vec{s}$, for the spin voltage $\vec{V}_s$ as they are directly proportional, $\vec{s} = \sigma/q\,D\vec{V}_s$. Substituting into (14) and (15) and using the tensor representations for $\overline{I}_s$ and $\overline{V}_s$, we are left with

$$\mathbf{C}_s \frac{\partial \overline{V}_s}{\partial t} = \frac{\partial \overline{I}_s}{\partial x} - \mathbf{G}_s \overline{V}_s$$
$$\overline{I}_s = \sigma A \frac{\partial \overline{V}_s}{\partial x} + \frac{\mu I_C}{D} \overline{V}_s \tag{18}$$

where $\mathbf{C}_s$ and $\mathbf{G}_s$ are the capacitance and conductance per unit length matrices defined as

$$\mathbf{C}_s = \begin{bmatrix} C_e & 0 & 0 & 0 \\ 0 & C_q A & 0 & 0 \\ 0 & 0 & C_q A & 0 \\ 0 & 0 & 0 & C_q A \end{bmatrix}$$
$$\mathbf{G}_s = \begin{bmatrix} 0 & 0 & 0 & 0 \\ 0 & \frac{C_q A}{\tau_s} & 0 & 0 \\ 0 & 0 & \frac{C_q A}{\tau_s} & 0 \\ 0 & 0 & 0 & \frac{C_q A}{\tau_s} \end{bmatrix} \tag{19}$$

Simplifying the analysis of the drift–diffusion equations requires an approximation of the spatial derivative, ∂x. The finite-difference method is applied to the drift–diffusion equation to approximate a nonmagnetic conductor of length L. The finite-difference approximation $\partial/\partial x \Rightarrow \Delta/\Delta x$ results in N number of drift–diffusion equations, each for a conductor segment of length $\Delta x = L/N$. The segments of length Δx cause a difference in voltage of $\Delta\overline{V}_s = \Delta\overline{V}_s(x) - \Delta\overline{V}_s(x + \Delta x)$ and a change in current of $\Delta\overline{I}_s = \Delta\overline{I}_s(x) - \Delta\overline{I}_s(x + \Delta x)$.

Each segment in a nonmagnetic conductor is represented using a circuit model. The circuit model is derived by solving for $\overline{I}_s$ and $\Delta\overline{I}_s$. The complete circuit model for spin transport (Fig. 3) consists of cascaded segments for each component of the $\overline{V}_s$ and $\overline{I}_s$ tensors.

III. Results

Compact circuit models should accurately predict the physical behavior of the system of interest. Circuit simulations of spintronic device models are presented to validate their accuracy. Analytical and numerical solutions of the governing physical equations form a basis for comparison. The results obtained using circuit simulation are compared with solutions of the physical equations used to derive the device models.

A. Thermal Noise Validation

The presence of thermal noise affects the transient characteristics of the magnetization dynamics. Thermal noise is caused by the thermally agitated motion of electrons in the ferromagnet [20]. Thermal noise leads to the presence of a thermal field, $\vec{H}_T$, in (5). An analytical solution exists for the steady-state precession angle, θ_0, based off of the formulas presented in [20] as a function of the ferromagnet temperature

$$\langle\theta_0^2\rangle = \frac{k_b T}{E_b}. \tag{20}$$

In Fig. 4, the ferromagnet model is simulated under varying temperatures, and the steady-state angle measured from SPICE matches the analytical solution within 5%.

B. LLG Equation Validation

The behavior of the LLG equation must be duplicated by the ferromagnet circuit model. Analytical solutions of the LLG equation are difficult to obtain and do not accurately represent all of the physical cases that will be encountered during circuit simulation [25]. The differential equation solver, LSODA [26], has been used to obtain numerical solutions of the LLG equation. The numerical simulation has been performed with the initial conditions $\vec{m}_i = [\,m_x = 1\ m_y = 0\ m_z = 0\,]^T$ and boundary conditions $\vec{I}_s = [\,I_{s,x} = 3mA\ I_{s,y} = 0mA\ I_{s,z} = 0mA\,]^T$, in the absence of thermal noise. In Fig. 5, the ferromagnet circuit model was simulated under identical conditions, and the results obtained from SPICE match identically with the results obtained from the LSODA simulation.

1) Ferromagnet Switching Time: The switching delay of a ferromagnet has been computed in [18] using the small cone-angle approximation. The delay, τ_{sw}, according to the small cone-angle approximation is

$$\tau_{sw} = \frac{M_s V q}{I_{s,\mathrm{cr}} \mu_b} \frac{\log \pi/\theta_0}{\chi - 1} \tag{21}$$

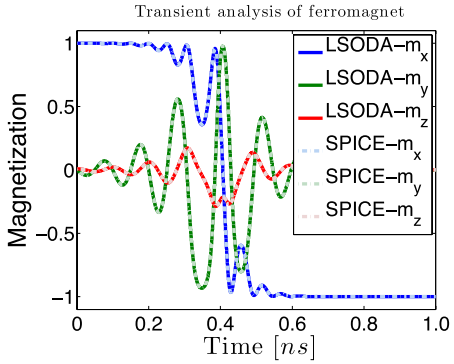

Fig. 5. Ferromagnet transient analysis (without thermal noise).

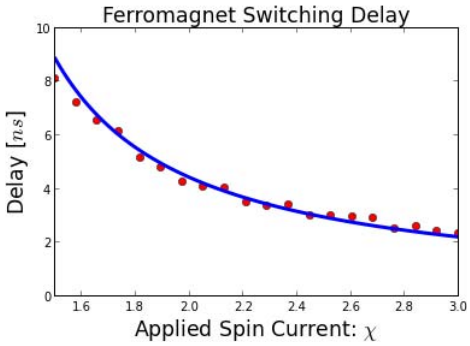

Fig. 6. Ferromagnet switching delay. A spin current of $\chi I_{s,\mathrm{cr}}$ is applied to the ferromagnet and the resulting switching delay is measured. Red symbols: the circuit simulations. Blue curve: the analytical solution.

where $\chi I_{s,\mathrm{cr}}$ is the magnitude of the applied spin current. Since this equation is for perpendicular ferromagnets with uniaxial anisotropy only, we have simplified the effective magnetic field, $\vec{H}_{\mathrm{eff}}$, to reflect this. Equation (21) can then be used as an additional method for validating the compact circuit model. The comparison with the SPICE simulations is shown in Fig. 6.

C. Validation of Spin Drift–Diffusion

The spatial discretization is the key assumption that enables the development of the spin transport circuit model. The analytical solution of the steady-state case provides an accurate solution of the spatial propagation of the spin voltage [24], therefore making it a suitable formula for validating the finite-difference approximation used by the circuit model. In Fig. 7, the circuit simulations of the spin transport model accurately predict the spatial propagation of the spin voltage within 1% of the analytical solution for the steady-state case.

D. Case Studies

1) All-Spin Logic Device Simulation: Combining the compact models for spin storage, spin transport, and spin injection enables the cosimulation of magnetization dynamics and spin transport dynamics. A useful application for these device models is in the simulation of an all-spin logic (ASL) device [4] that operates as a Boolean logic inverter. The complete equivalent circuit for such a device is shown in Fig. 8, where

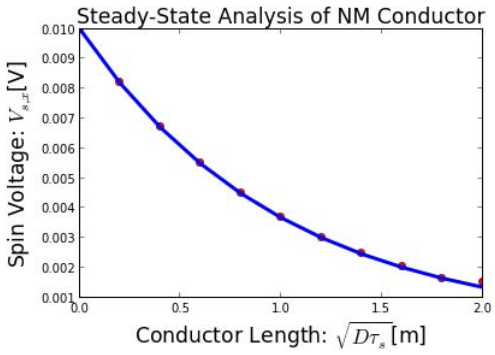

Fig. 7. Nonmagnetic conductor steady-state analysis. Red symbols: the circuit simulations. Blue curve: the analytical solution. x-axis: the length relative to the spin diffusion length, $L_s = \sqrt{D\tau_s}$.

we have combined the compact models for the magnetization dynamics, spin injection, and spin transport.

In Fig. 9, an ASL device is driven by a 100-mV pulse. When the supply is $+100$ mV, the device behaves as an inverter, and the output magnet switches to the opposite state of the input magnet. When the supply is -100 mV, the output performs the opposite operation and copies the state of the input magnet.

2) ASL Majority Gate: The compact circuit models enable the design of other ASL circuits capable of other Boolean logic functions. An example circuit is shown in the inset of Fig. 10, where we have constructed a device that behaves as a majority gate capable of the Boolean NAND and NOR operations. The magnets $\vec{m}_A$ and $\vec{m}_B$ serve as inputs, while $\vec{m}_C$ is used to bias the device as a NAND or NOR gate. When the bias magnet is configured in the $-x$-direction, the device behaves as a NAND gate. When biased in the $+x$-direction, the device functions as a NOR gate. The transient simulation of the ASL majority gate is shown in Fig. 10 for both the NAND and NOR functions.

IV. Discussion

To prove the validity of the models presented in this paper, comparisons with the underlying physical equations are necessary. A numerical solution of the LLG equation was found to match the simulation results of the ferromagnet device model. An analytical solution of the spin drift–diffusion equation was used to verify the accuracy of the discretization method that enabled the development of the spin transport compact model. Test cases and properties of the compact models were shown and discussed to demonstrate the capabilities enabled by the compact models.

The behavior of a ferromagnet under varying spin currents and applied field conditions was predicted in [18]. The formulas presented in [18] for the delay, τ_{sw}, and the critical current, $I_{s,\mathrm{cr}}$, predict the overall behavior of a ferromagnet under switching conditions. These characteristics were observed using the ferromagnet circuit model developed in this paper. In addition, the combined spintronic models used in the ASL inverter shown in Fig. 9 under positive and negative bias voltages match what was anticipated in [27]. This demonstrates the successful operation of a spintronic device

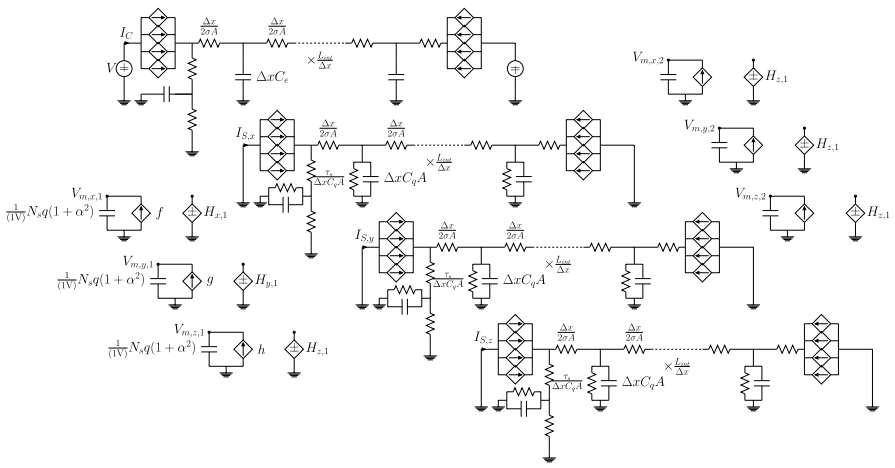

Fig. 8. ASL circuit model.

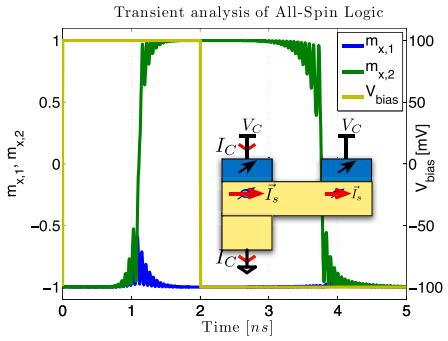

Fig. 9. ASL transient analysis.

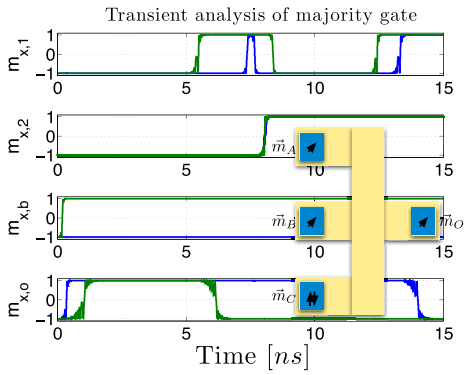

Fig. 10. Majority gate transient analysis. Blue: NAND. Green: NOR.

using circuit simulation of the magnetization dynamics and spin transport physics.

The circuit models in this paper map the physical equations of spintronic devices to circuit components prevalent in digital circuit design. The capacitor present in the ferromagnet model plays a significant role in determining the transient characteristics of the magnetization dynamics, clearly highlighting the importance of the product $qN_s(1+\alpha^2)$ present in the LLG equation. The shunt resistance present in the spin transport model illustrates the importance of the ratio $\tau_s C_q A \Delta x$ in determining the channel length limits of spintronic devices. This creates an important connection between the material parameters present in the physical equations and the performance of spintronic devices. Circuit designers can also utilize the device models, since a complicated device, such as the NAND/NOR majority gate, can be created by treating the spintronic device as a block-level design instead of a more complicated set of spin physical equations. Future works might seek to develop an understanding of spintronic devices based on the circuit components used in the equivalent circuits developed in this paper.

V. Conclusion

We have successfully developed and validated compact models for spintronic devices. These models enable the cosimulation of the magnetization dynamics and spin transport physics necessary to simulate spintronic devices. Using these models, we simulated the operation of the ASL device using circuit simulation. This enables the study of ASL devices using circuit design tools and is essential to the design process of future spintronic devices.

Appendix

Circuit Parameters

The following list includes all of the necessary parameters for the compact models presented in this paper. The interface parameters include the two-channel conductances, $G_\uparrow$ and $G_\downarrow$, and the mixing conductance, $G_{\uparrow\downarrow}$. The ferromagnet parameters include the dimensions, L_x, L_y, and L_z, the saturation magnetization, M_s, and the Gilbert damping coefficient, α. The remaining ferromagnet parameters are a function of these, and we have referenced the relevant works for their calculation in the case of a cobalt ferromagnet. The channel parameters include the dimensions, length (L_{int}), width (W_{int}), and the thickness-to-width aspect ratio (AR), in addition to the material parameters calculated in [28] for a copper channel.

1) *Interface Parameters (Co/Cu) [14]:* $G_\uparrow = 0.600$ 1/Ω, $G_\downarrow = 0.514$ 1/Ω, $\text{Re}G_{\uparrow\downarrow} = 1.717$ 1/Ω, and $\text{Im}G_{\uparrow\downarrow} = 0.025$ 1/Ω.

2) *Ferromagnet (Co) [19], [25]:* $L_x = 75.60$ nm, $L_y = 37.80$ nm, $L_z = 3.00$ nm, $\alpha = 0.01$, $\gamma = 17.60 \times 10^{10}$ 1/sT, $M_s = 1.45 \times 10^{06}$ A/m, $N_s = 1.34 \times 10^{06}$, $1/(1V)N_s q(1+\alpha^2) = 214.72$ fF, $K_u = 0.5 \times 10^5$ J/m^2, $N_x = 0.044$, $N_y = 0.091$, and $N_z = 0.864$.
3) *Channel (Cu) [28]:* $L_{\text{int}} = 100.0$ nm, $W_{\text{int}} = 100.0$ nm, AR $= 2.0$, $H_{\text{int}} = W_{\text{int}}/\text{AR} = 50.0$ nm, $A = W_{\text{int}} H_{\text{int}} = 5000.0$ nm^2, $\Delta x = 10.0$ nm, $\sigma = 41.549$ $1/\mu\Omega$m^2, $D = 0.014$ m^2/s, $\mu = 0.003$ m^2/Vs, $\tau_s = 10.939$ ps, $R_s = \Delta x/2\sigma A = 0.024$ Ω, $R_{s,\text{shunt}} = D\tau_s/\sigma A \Delta x = 74.982$ Ω, and $C_s = \sigma A \Delta x/D = 145.890$ fF.

REFERENCES

[1] S. Srinivasan, A. Sarkar, B. Behin-Aein, and S. Datta, "All-spin logic device with inbuilt nonreciprocity," *IEEE Trans. Magn.*, vol. 47, no. 10, pp. 4026–4032, Oct. 2011.

[2] I. Žutić, J. Fabian, and S. Das Sarma, "Spintronics: Fundamentals and applications," *Rev. Mod. Phys.*, vol. 76, pp. 323–410, Apr. 2004.

[3] J. Slonczewski, "Current-driven excitation of magnetic multilayers," *J. Magn. Magn. Mater*, vol. 159, nos. 1–2, pp. L1– L7, 1996.

[4] B. Behin-Aein, D. Datta, S. Salahuddin, and S. Datta, "Proposal for an all-spin logic device with built-in memory," *Nature Nanotechnol.*, vol. 5, no. 4, pp. 266–270, 2010.

[5] E. I. Rashba, "Theory of electrical spin injection: Tunnel contacts as a solution of the conductivity mismatch problem," *Phys. Rev. B*, vol. 62, pp. R16267–R16270, Dec. 2000.

[6] F. Mireles and G. Kirczenow, "From classical to quantum spintronics: Theory of coherent spin injection and spin valve phenomena," *Europhys. Lett.*, vol. 59, no. 1, pp. 107–113, 2002.

[7] S. Das Sarma, J. Fabian, X. Hu, and I. Zutic, "Theoretical perspectives on spintronics and spin-polarized transport," *IEEE Trans. Magn.*, vol. 36, no. 5, pp. 2821–2826, Sep. 2000.

[8] I. Zutic, J. Fabian, and S. Erwin, "Bipolar spintronics: Fundamentals and applications," *IBM J. Res. Develop.*, vol. 50, no. 1, pp. 121–139, 2006.

[9] L. Berger, "Emission of spin waves by a magnetic multilayer traversed by a current," *Phys. Rev. B*, vol. 54, pp. 9353–9358, Oct. 1996.

[10] L. D. Landau and E. Lifshitz, "On the theory of the dispersion of magnetic permeability in ferromagnetic bodies," *Phys. Z. Sowjetunion*, vol. 8, no. 153, pp. 101–114, 1935.

[11] T. Gilbert and J. Kelly, "Anomalous rotational damping in ferromagnetic sheets," in *Proc. Conf. Magn. Magn. Mater.*, Pittsburgh, PA, USA, 1955, pp. 253–263.

[12] T. Valet and A. Fert, "Theory of the perpendicular magneto resistance in magnetic multilayers," *Phys. Rev. B*, vol. 48, pp. 7099–7113, Sep. 1993.

[13] A. Brataas, Y. V. Nazarov, and G. E. W. Bauer, "Finite-element theory of transport in ferromagnet-normal metal systems," *Phys. Rev. Lett.*, vol. 84, pp. 2481–2484, Mar. 2000.

[14] A. Brataas, G. E. Bauer, and P. J. Kelly, "Non-collinear magnetoelectronics," *Phys. Rep.*, vol. 427, no. 4, pp. 157–255, 2006.

[15] G. Panagopoulos, C. Augustine, and K. Roy, "A framework for simulating hybrid MTJ/CMOS circuits: Atoms to system approach," in *Proc. DATE*, 2012, pp. 1443–1446.

[16] B. Behin-Aein, A. Sarkar, S. Srinivasan, and S. Datta, "Switching energy-delay of all spin logic devices," *Appl. Phys. Lett.*, vol. 98, no. 12, pp. 123510-1–123510-3, 2011.

[17] T. Quarles, A. Newton, D. Pederson, and A. Sangiovanni-Vincentelli, *SPICE 3 User Manual*. Berkeley, CA, USA: Univ. California, 1993.

[18] J. Z. Sun, "Spin-current interaction with a monodomain magnetic body: A model study," *Phys. Rev. B*, vol. 62, pp. 570–578, Jul. 2000.

[19] M. Beleggia, M. D. Graef, and Y. T. Millev, "The equivalent ellipsoid of a magnetized body," *J. Phys. D, Appl. Phys.*, vol. 39, no. 5, p. 891, 2006.

[20] W. Brown, "Thermal fluctuation of fine ferromagnetic particles," *IEEE Trans. Magn.*, vol. 15, no. 5, pp. 1196–1208, Sep. 1979.

[21] S.-F. Lee, W. P. Holody, Q. Yang, P. Holody, R. Loloee, P. Schroeder, *et al.*, "Two-channel analysis of CPP-MR data for Ag/Co and AgSn/Co multilayers," *J. Magn. Magn. Mater.*, vol. 118, nos. 1–2, pp. L1–L5, 1993.

[22] K. Xia, P. J. Kelly, G. E. W. Bauer, A. Brataas, and I. Turek, "Spin torques in ferromagnetic/normal-metal structures," *Phys. Rev. B*, vol. 65, no. 22, pp. 220401-1–220401-4, May 2002.

[23] J. Fabian and S. Das Sarma, "Spin relaxation of conduction electrons in polyvalent metals: Theory and a realistic calculation," *Phys. Rev. Lett.*, vol. 81, pp. 5624–5627, Dec. 1998.

[24] J. Fabian, A. Matos-Abiague, C. Ertler, P. Stano, and I. Žutić, "Semiconductor spintronics," *Acta Phys. Slovaca*, vol. 57, pp. 565–907, Aug. 2007.

[25] J. Xiao, A. Zangwill, and M. D. Stiles, "Macrospin models of spin transfer dynamics," *Phys. Rev. B*, vol. 72, pp. 014446-1–014446-13, Jul. 2005.

[26] A. C. Hindmarsh, *ODEPACK, a Systematized Collection of ODE Solvers*, vol. 1, R. S. Stepleman, *et al.*, Eds. New York, NY, USA: Amsterdam, 1983, pp. 55–64.

[27] B. Behin-Aein and S. Datta, "All-spin logic," in *Proc. Device Res. Conf.*, 2010, pp. 41–42.

[28] S. Rakheja, S.-C. Chang, and A. Naeemi, "Impact of dimensional scaling and size effects on spin transport in copper and aluminum interconnects," *IEEE Trans. Electron Devices*, vol. 60, no. 11, pp. 3913–3919, Nov. 2013.

Phillip Bonhomme (M'14) received the M.S. degree in electrical and computer engineering from the Georgia Institute of Technology, Atlanta, GA, USA.

He is currently a Hardware Engineer with Intel Corporation, Hillsboro, OR, USA.

Sasikanth Manipatruni received the B.S. degree in electrical engineering from IIT Delhi, Delhi, India, and the Ph.D. degree in electrical and computer engineering from Cornell University, Ithaca, NY, USA.

He is a Staff Scientist with the Exploratory Integrated Circuits Group, Components Research Intel, Hillsboro, OR, USA, involved in beyond CMOS devices and circuits.

Rouhollah M. Iraei received the B.S. degree in electrical engineering from Sharif University, Tehran, Iran, in 2012. He is currently pursuing the Ph.D. degree in electrical and computer engineering with the Georgia Institute of Technology, Atlanta, GA, USA.

Shaloo Rakheja received the M.S. and Ph.D. degrees in electrical and computer engineering from the Georgia Institute of Technology, Atlanta, GA, USA, in 2009 and 2012, respectively.

She is currently a Post-Doctoral Associate with the Microsystems Technology Laboratories, Massachusetts Institute of Technology, Cambridge, MA, USA.

Sou-Chi Chang received the B.S. degree in electrical engineering from the National Chiao Tung University, Hsinchu, Taiwan, and the M.S. degree in electrical engineering and computer science from the University of Michigan, Ann Arbor, MI, USA, in 2008 and 2011, respectively. He is currently pursuing the Ph.D. degree in electrical and computer engineering with Georgia Institute of Technology, Atlanta, GA, USA.

Dmitri E. Nikonov (M'99–SM'06) received the M.S. degree in aeromechanical engineering from the Moscow Institute of Physics and Technology, Moscow, Russia, and the Ph.D. degree in physics from Texas A&M University, College Station, TX, USA, in 1992 and 1996, respectively.

He is currently a Principal Engineer with the Components Research Group, Hillsboro, OR, USA, involved in simulation and benchmarking of beyond-CMOS logic devices.

Ian A. Young (M'78–SM'96–F'99) received the B.S. degree in electrical engineering and the M.Sc.Eng. degree from the University of Melbourne, Melbourne, VIC, Australia, and the Ph.D. degree in electrical engineering and computer science from the University of California, Berkeley, CA, USA.

He is a Senior Fellow with the Technology and Manufacturing Group, Intel Corporation, Santa Clara, CA, USA.

Azad Naeemi (S'99–M'04–SM'04) received the B.S. degree in electrical engineering from Sharif University, Tehran, Iran, and the M.S. and Ph.D. degrees in electrical and computer engineering from the Georgia Institute of Technology (Georgia Tech), Atlanta, GA, USA, in 1994, 2001, and 2003, respectively.

He is currently an Associate Professor with the School of Electrical and Computer Engineering, Georgia Tech.